

Design of a Large-Bore 60-T Pulse Magnet for Sandia National Laboratories

L. Li (1), D. Rovang (2), B. Lesch (1), P. Pernambuco-Wise (3) and H. J. Schneider-Muntau (1)
 (1) National High Magnetic Field Laboratory, 1800 E Paul Dirac Drive, Tallahassee, FL, USA
 (2) Sandia National Labs*, Albuquerque NM, USA
 (3) Oceanit Laboratories Inc. Honolulu, Hawaii, USA

RECEIVED
 OCT 20 1999
 OSTI

Abstract--

The design of a new pulsed magnet system for the generation of intense electron beams is presented. Determined by the required magnetic field profile along the axis, the magnet system consists of two coils (Coil #1 and #2) separated by a 32-mm axial gap. Each coil is energized independently. Both coils are internally reinforced with HM Zylon fiber/epoxy composite. Coil #1 made with Al-15 Glidcop wire has a bore of 110-mm diameter and is 200-mm long; it is energized by a 1.3-MJ, 13-kV capacitor bank. The magnetic field at the center of this coil is 30 T. Coil #2 made with CuNb wire has a bore of 45 mm diameter, generates 60 T with a pulse duration of 60 ms, and is powered by a 4.0-MJ, 17.7-kV capacitor bank. We present design criteria, the coupling of the magnets, and the normal and the fault conditions during operation.

I. INTRODUCTION

Sandia National Labs is investigating and developing high-dose high-brightness flash radiographic sources. One of the sources being developed is the magnetically-immersed electron diode. A high voltage (up to 20 MV), high current (10s of kA), pulse (10s of nanoseconds) is applied to the diode by an Inductive Voltage Adder (IVA) accelerator [1]. Electrons are drawn from the needle like cathode (< 1-mm diameter) and accelerated toward the anode target. The target, typically a high Z material such as tantalum, converts the electron beam into an intense x-ray beam. Ion-emitting plasmas can form on the target and surrounding anode surfaces due to direct beam heating and radiation emitted from the target. These ions can have deleterious effects on the generation of an intense electron beam. Previous experiments [2] and theoretical understanding [3] resulting from those experiments have suggested that successful operation of the diode and generation of small electron beams (~1-mm dia.) will require a stepped magnetic field configuration like that shown in Figure 1 to mitigate these effects. In this stepped configuration, the cathode needle terminates in the middle of the large 110-mm bore, while the target is located at middle of the small 45-mm bore. The magnetic field strength increases monotonically from 30 T at the cathode needle tip to 60 T at the target. In this paper, we describe

the design and operation of the magnet system under both normal and fault conditions.

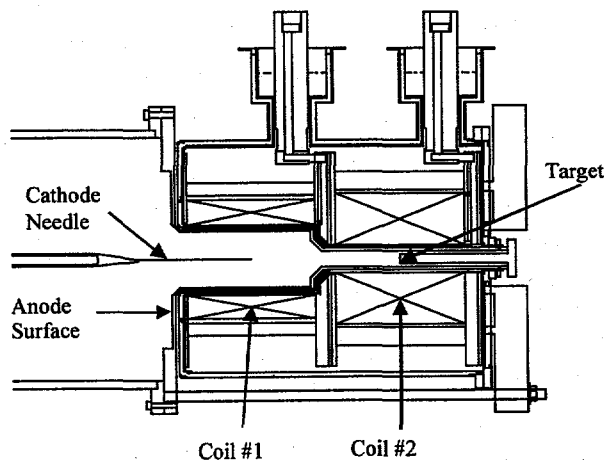


Figure 1. Magnetically immersed diode. The coils shown are wire wound internally reinforced, liquid nitrogen cooled magnets. The large bore magnet is a 30-T, 110-mm diameter coil made with Al-15 Glidcop wire and HM Zylon reinforcement. The small-bore magnet is 60-T, 45-mm diameter coil made with CuNb wire and HM Zylon reinforcement.

II. MAGNET DESIGN

In order to provide the required magnetic field profile, the magnet is designed to be composed of two coils as shown in Figure 1. Parameters of the two coils are given in Table 1. Both coils are pre-cooled with liquid nitrogen and are energized with their own capacitor bank.

Coil #1 with a bore of 110-mm diameter is made from Glidcop Al-15 conductor wire with a rectangular cross section (4 mm x 6 mm). The Glidcop Al-15 wire has an ultimate tensile strength of about 530 MPa at room temperature and 660 MPa at 77 K at an elongation of about 12%. HM (high modulus) Zylon fiber composite is used for optimized internal reinforcement and a stainless steel shell over-wrapped with Zylon fiber as external reinforcement. The fiber has a modulus of 280 GPa with a tensile strength of 5.8 GPa and its elongation at break is 2.5%. The packing factor of this fiber wound using the

* Sandia is a multi-program laboratory operated by Sandia Corporation, a Lockheed Martin Company, for the United States Department of Energy under Contract DE-AC04-94AL85000.

DISCLAIMER

This report was prepared as an account of work sponsored by an agency of the United States Government. Neither the United States Government nor any agency thereof, nor any of their employees, make any warranty, express or implied, or assumes any legal liability or responsibility for the accuracy, completeness, or usefulness of any information, apparatus, product, or process disclosed, or represents that its use would not infringe privately owned rights. Reference herein to any specific commercial product, process, or service by trade name, trademark, manufacturer, or otherwise does not necessarily constitute or imply its endorsement, recommendation, or favoring by the United States Government or any agency thereof. The views and opinions of authors expressed herein do not necessarily state or reflect those of the United States Government or any agency thereof.

DISCLAIMER

Portions of this document may be illegible in electronic image products. Images are produced from the best available original document.

coil-winding machine at NHMFL could be above 80 %. Vacuum impregnation of the Zylon fiber at such a high packing factor is difficult. When using it as internal reinforcement, wet winding is more practical. The HM Zylon fiber is selected as the internal reinforcing material because of its high strength and high Young's modulus, which will improve magnet lifetimes by reducing the strain cycle of the conductor during the pulse. The power supply of the 30-T, 110-mm bore magnet is a 16-mF, 15-kV capacitor bank. Discharging the capacitor bank at 13 kV, Coil #1 can provide 27.5 T at its center with a pulse duration 30 ms. This together with the magnetic field contributed from Coil #2 produces 30 T at the coil center.

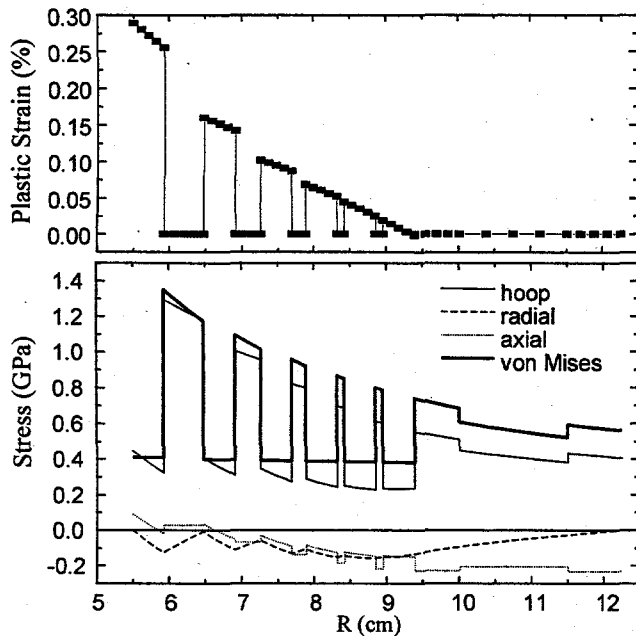


Figure 2. Stress and plastic strain distribution in the mid-plane of Coil #1 at 27 T in a background field of 3 T.

The geometry of the coil #1 is listed in Table II. The magnet is 200-mm long, consisting of 6 layers of conductor with interleaving Zylon layers. A heavy external reinforcement prevents winding deformation [5]. A significant amount of stress is transmitted to the outer shell in coils with small OD/ID aspect ratios similar to Coil #1. Figure 2 shows the stress distribution in the mid-plane of the coil at 28 T with a 2-T background field. The coil will experience some plastic deformation during the initial training. After the training the coil will run in an elastic state because of the strain hardening.

The Coil #2 design is based on CuNb conductor produced by the Bochvar Institute in Russia. The wire has a tensile strength of 1.2 GPa with 3% elongation at room temperature and 1.35 GPa at 77 K. The wire conductivity is 70 % IACS and the resistance ratio is 4.6. The excellent properties of this material will certainly make a valuable contribution to high field pulsed magnet development. Short samples of such wires have been tested at NHMFL, which verified that the wire meets manufacturer

specifications. A conductor cross section of 4 mm x 6 mm was chosen, determined by the pulse duration and the allowable temperature rise. The inner six layers of conductors are internally reinforced by the HM Zylon fibers. The magnet geometry is listed in Table II. The thickness of the internal reinforcement of each layer is adjusted to evenly distribute the stress in the reinforcement across the six layers. This limits the highest strain in the conductors below 1.1%. The coil will undergo less than 0.1% plastic strain during the initial training of the coil and will then run in the elastic state. The outer shell of A286 and Zylon limits the strain in the six outer layers of the coil. Zylon fiber is placed between those layers to transmit the stress and provide additional insulation. The stress and strain distribution in Coil #2 is shown in Figure 3. The plastic deformation in the conductors is so small that the stress and plastic strain in the conductor is lower than its proof values. The 15-mm thick A286 stainless steel provides stiffness in the axial and radial direction.

Table I. The main parameters of the two coils

	Coil #1	Coil #2	units
Peak field at center	30	60	Tesla
Inner diameter	110	45	mm
Length	200	200	mm
Number of layers	6	12	layers
Coil inductance	2.27	5.77	mH
Capacitance energy	1.3	4	MJ
Voltage	13000	17700	volts
Leading resistance	40	40	mOhm
Leading inductance	10	10	μ H
Crowbar resistance	250	380	mOhm
Mutual inductance	0.37	0.37	mH
Peak current	29600	30100	A
Rise time	9	17	ms

Table II. Parameters of the magnets and their power supplies.

layer	Coil #1		Coil #2	
	Wire thickness	Reinf thickness (mm)	Wire thickness (mm)	Reinf. thickness (mm)
1	3.2	5.5	3.2	3.1
2	3.2	3.5	3.2	3.9
3	3.2	2.0	3.2	4.7
4	3.2	1.0	3.2	5.3
5	3.2	1.0	3.2	5.7
6	3.2	6.2	3.2	0.8
7		15 A286	3.2	0.5
8		7.5	3.2	0.5
9			3.2	0.5
10			3.2	0.5
11			3.2	0.5
12			3.2	5.9
13				15 (A286)
14				20

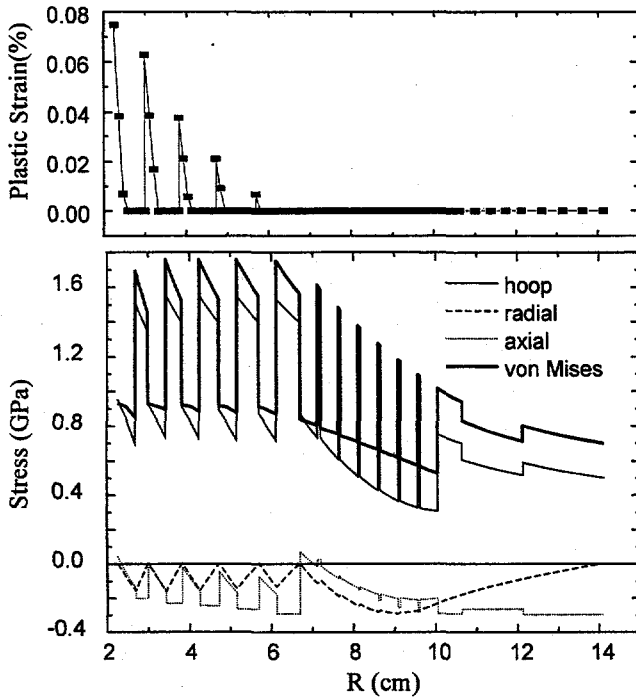


Figure 3. Stress and the plastic strain distribution in Coil #2 at 58 T with a background field of 2 T.

The axial separation between the two coil windings is 32 mm. This gap provides the desired magnetic field axial profile as shown in Figure 4. This gap will be filled with a G10 plate, which needs to be strong enough to withstand the compression of the two magnets due to the magnetic attraction.

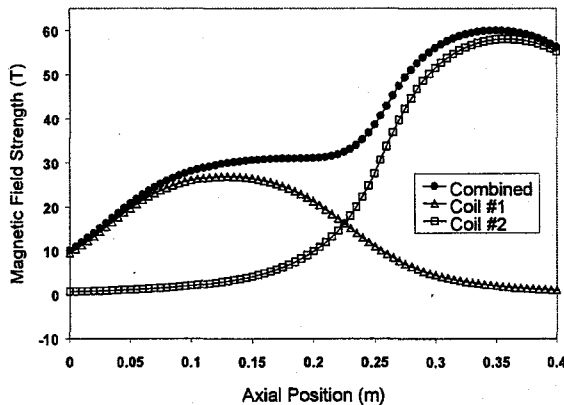


Figure 4. Magnetic profile along the axis of the system with a 32-mm gap between the two coil windings.

III. ELECTRICAL PERFORMANCE OF THE COUPLED MAGNET SYSTEM

An LRC-circuit with constant parameters does not adequately describe the discharge. Both the resistance and

the inductance of the magnet vary as a function of time due to the temperature rise of the wire, the skin effect, and the magneto-resistance. For a system of magnetically and electrically coupled circuits energized by different power supplies, the equation for each circuit can be written as:

$$\frac{d^2 I_i}{dt^2} = \frac{1}{L_i} \left(\frac{I - I_c}{C_i} - R_i \frac{dI_i}{dt} - I_i \frac{dR_i}{dt} + \frac{dV_m}{dt} + \frac{dV_e}{dt} \right) \quad (1)$$

where L_i , R_i and C_i are the inductance, resistance and the capacitance of circuit i respectively. The induced voltage V_m representing the coupling of the circuit with the others and it can be expressed as

$$V_m(i) = \sum M(i, j) \frac{dI(j)}{dt}, \quad (2)$$

with $M(i, j)$ the mutual inductance between circuit i and circuit j , which can be calculated from their relative positions and the coil geometry. The V_e in the Equation (1) reflects the coupling of the circuit with all the magnetic flux generated by the eddy current loops. This can be calculated by magnetic diffusion analysis [5].

A computer code has been developed for this purpose, solving the differential equations for each circuit with the Runge-Kutta method. The inductive voltage $V_m(i)$ due to the coupling between each circuit and all the other circuits is based on the current derivatives at the end of the previous time step. By solving the coupled circuit equations, the magnetic and thermal diffusions in a pulsed magnet system are calculated, from this the local temperature increase is determined.

Figure 5 shows the magnetic field axial waveform of the two-magnet system calculated from the capacitor bank parameters listed in Table 1. As a comparison the waveforms of the magnetic field generated in the independent operation are also shown in the figure with dashed and dotted lines. Due to the magnetic coupling, the waveform of each coil is deformed. In this particular case, the peak field is reduced from the 28 T to 26.9 T for coil #1 and 60.1 T to 57.7 T for Coil #2. The temperature distribution in both coils at the end of the pulse is shown in Figure 6.

The magnetic field waveform strongly depends on the time at which Coil #1 is switched on. If it is switched on during the upswing of the outer coil field, the peak fields of both coils reduce. If a magnet is fired during the downswing of field of the other, the coupling will increase current (thus the field) of this coil significantly while a dip will occur in the other field waveform. This is one of the fault conditions that need to be analyzed, and the electric circuit should prevent this from occurring. Another fault condition is if one of the coils does not fire. In this case, the other coil may produce a higher current and a higher field as we see

from Figure 5. This may damage the magnet by stress and heating. The magnets should be designed to survive this fault condition.

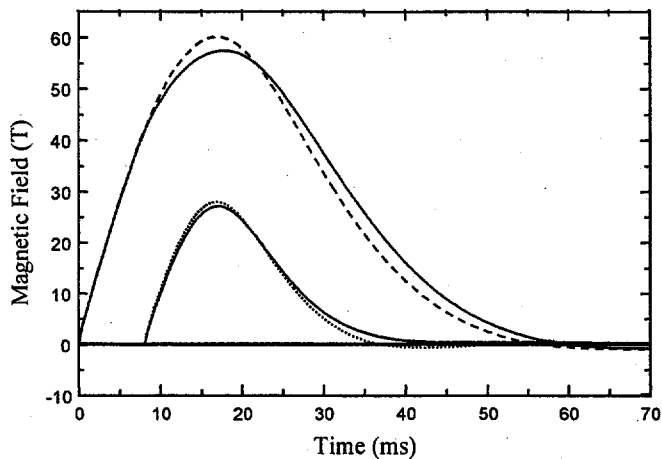


Figure 5. Computer simulated magnetic field waveforms of coils #1 and #2. The solid lines show the case when with the coupling of the two coils considered; while the dashed and dotted line represent the independent waveforms when the coils are energized with the same power supply.

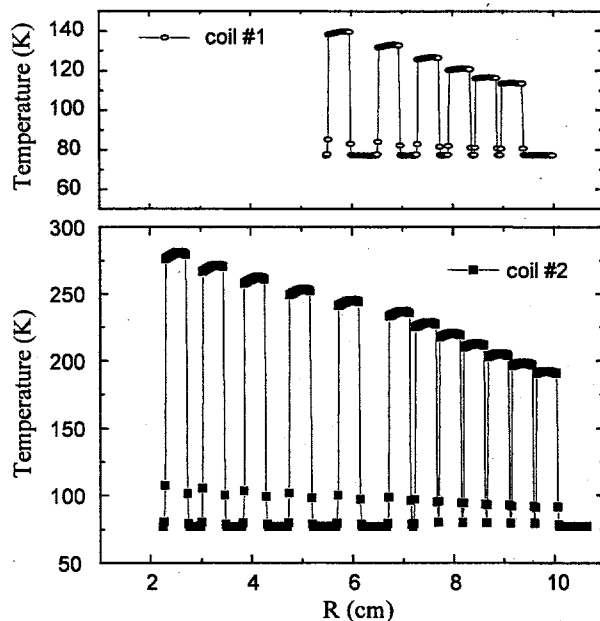


Figure 6. Temperature distribution at the end of the pulse in Coil #1 and #2.

IV. CONCLUSIONS AND THE PROJECT STATUS

The design of the combination of a 45-mm bore 60-T and a 110-mm bore 30-T magnet system has been presented, which shows a promising performance. The mechanical and electrical analyses have been carried out with a developed computer program. This is new and unique high field pulsed magnet system, which involves high voltage (18 kV), high energy (5.3 MJ), magnetic coupling, new

materials and new technology. To gain experience for both magnet engineers and the application physicists, a 50-T prototype system will be built first and used for the preliminary experiments. As the CuNb wire is still under development, the 50 T magnet will be made from the 4-mm x 6-mm Glidcop conductor. We will first build and test the 30 T magnet in January and the 50 T magnet in March of next year. The combined system will be tested in May 2000. When these tests are complete, the system will be upgraded with the CuNb wire based on the design described in this paper and the experience gained during the development of the prototype coils.

References

1. J. Maenchen et al., "Inductive Voltage Adder Driven X-ray Sources for Hydrodynamic Radiography," 12th IEEE Int. Pulsed Power Conference, Monterey, CA, Jun3 27-30, 1999.
2. M. G. Mazarakis et al., *Appl. Phys. Lett.* **70**, 832, 1997.
3. D. R. Welch et al., "Theoretical Support for the Inductive-Voltage-Adder Radiography Program at Sandia National Laboratories," Mission Research Report #MRC/ABQ-R-1889, September 1998.
4. L. Li and F. Herlach, "Deformation Analysis of Pulsed Magnets with Internal and External Reinforcement," *Meas. Sci. and Tech.*, **6** (1995), 1035-1042.
5. L. Li and F. Herlach, "Magnetic and Thermal Diffusion in Pulsed High-Field Magnets," *Journal of Physics D-Applied Physics* **31**, (11) 1320-1328 (1998)